Work input and launch height of an elastomeric popper: a quantitative study

Rohan Armand Andreu Dela Rosa,* Mason Levine, and Deven Khettry
Science & Engineering Magnet Program, Manalapan High School, Englishtown, NJ 07726 USA
(Received 29 January 2026; accepted 11 April 2026; published 17 May 2026)

This study quantifies the relationship between mechanical work applied during compression of an elastomeric popper and the maximum height achieved at launch. Five compression depths (1.0 cm to 4.5 cm) were each replicated three times, yielding 15 trials total. Work input was determined via trapezoidal Riemann sums of force-displacement data collected with a calibrated scissor jack and digital force gauge. Initial launch velocity was extracted frame-by-frame using Tracker video analysis software (60 frame/s), and maximum height was measured optically against a calibrated scale. Results show strong positive linear correlations between work input and both launch kinetic energy ($R^2 = 0.998$) and peak gravitational potential energy ($R^2 = 0.997$). Across all compression levels, an average of $54 \pm 1\,\%$ of the compression work was lost prior to launch, consistent with published hysteresis losses for natural rubber under rapid inversion. The remaining 1 % conversion loss from kinetic to gravitational potential energy is attributed to aerodynamic drag and is consistent with a simple drag estimate. These results confirm the hypothesized positive correlation between work input and launch height and are quantitatively consistent with conservation of energy when dissipative mechanisms are properly accounted for.

DOI: 10.64808/9p4r7z72

I. INTRODUCTION

Elastomeric hemispherical shells, commonly marketed as toys called "poppers," serve as accessible laboratory models for studying energy storage and conversion. When mechanically inverted and compressed below their snap-through threshold, these devices store elastic strain energy [1, 2]. Right after the release, a rapid change in shape converts stored elastic potential energy into kinetic energy, pushing the shell vertically. The work-energy theorem says that the net work done on a system should equal the change in kinetic energy [3–5]. This implies that increasing the mechanical work input while we compress the popper should produce a relatively proportional increase kinetic energy at launch and, therefore, in maximum height attained by the popper.

A critical thing we need to consider is energy dissipation. Elastomeric materials exhibit hysteresis, so energy stored during deformation is not able to be completely recovered upon release, with a fraction of the energy being converted to thermal energy via friction [6, 7]. A secondary source of loss is acoustic emission during the snap event. During flight, aerodynamic drag removes a small additional fraction of kinetic energy. The goal of this study is to (1) confirm a positive correlation between work input and launch height across multiple independently varied compression levels, (2) measure the overall energy budget quantitatively, and (3) compare observed losses to published bounds.

FIG. 1. Scissor jack and scale

We hypothesized that maximum launch height would increase monotonically with work input, and that energy losses between compression work and launch kinetic energy would fall within the 70 % to 90 % range reported in the literature for rapid rubber inversion [7].

II. METHODS AND MATERIALS

A. Apparatus

An elastomeric popper (Liberty Imports; Allentown, PA; mass $m = 5.70 \pm 0.05$ g), measured on a digital balance) was used for all trials. Compression was applied using a scissor jack fitted with a flat aluminum plate to ensure uniform loading across the rim. The force of compression was measured with a digital scale (SmartWeigh; Jiangsu, China) mounted between the scissor jack and

* Contact author: 427rdelarosa@frhsd.com

the popper. Displacement was measured with a ruler. Two vertical meter sticks were placed to a wall and aligned in the camera's field of view to provide a height reference. Launches were recorded at 60 frame/s with a fixed iPhone camera (Apple; Cupertino, CA) placed 1.5 m from the apparatus at a horizontal distance sufficient to keep the entire trajectory in frame.

B. Compression work measurement

To quantify work input, a scissor jack compressed the popper against a digital scale (TOP2KG; Smart Weigh; Jiangsu, China). For all of the five compression depths (1.0 cm, 2.0 cm, 3.0 cm, 4.0 cm and 4.5 cm), the scissor jack was advanced in 1 cm then 0.5 cm increments and we measured the force. Each full force-displacement curve was replicated three times on separate times to see if we could reproduce the measurements. The total mechanical work W for each compression depth was calculated using a trapezoidal Riemann sum [8]:

$$W = \sum \frac{1}{2}(F_i + F_{i+1})(\Delta x) \tag{1}$$

where F_i is the force at displacement step i and $\Delta x = 0.005\,\text{m}$. All force values were recorded directly in N from the gauge display; no unit conversions were required.

C. Launch velocity and height analysis

Video files were imported into Tracker (Open Source Physics, v6.1.5) and calibrated using the known meter-stick spacing [9, 10]. Methods for obtaining launch kinematics were similar to [11–16]. Initial launch velocity v_0 was determined by tracking the centroid of the popper across three consecutive frames immediately after liftoff (frames 1–3 post-release), yielding two independent velocity estimates that were averaged. Peak height was seen as the frame in which the popper's top reached its maximum vertical level before it started to fall down. This was seen against the meter-stick background in the same frame. All distances are reported in m.

D. Energy calculations

Initial kinetic energy (KE) and peak gravitational potential energy (GPE) were calculated independently using [3–5]:

$$KE = \frac{1}{2}mv_0^2, \tag{2}$$

$$GPE = mgh, \tag{3}$$

TABLE I. Force-displacement data, $n = 3$ replicates

x, m	F, N		
0.000	0.0	0.1	0.0
0.005	1.2	1.5	1.4
0.010	2.7	3.1	2.9
0.015	4.4	4.0	4.2
0.020	5.3	5.9	5.8
0.025	7.5	7.0	7.1
0.030	6.5	7.1	6.8
0.035	5.3	6.0	5.7

where $m = 0.0057\,\text{kg}$ and $g = 9.81\,\text{m s}^{-2}$. KE and GPE were calculated independently from v_0 and h respectively; neither was derived from the other. The energy retained from compression to launch was computed as

$$\eta = \frac{\text{KE}_0}{W} \times 100\,\%. \tag{4}$$

A paired t-test ($\alpha = 0.05$ significance level) was used to compare work input to GPE at peak height across the 15 individual trials [17–20].

E. Drag estimation

Work done by drag during flight was estimated using the following relationships [3, 5]:

$$F_{drag} \approx 0.5\rho C_D A v_{avg}^2, \tag{5}$$

$$W_{drag} \approx F_{drag} h, \tag{6}$$

where $\rho = 1.20\,\text{kg m}^{-3}$, $C_D = 0.47$, $A = 7.1 \times 10^{-4}\,\text{m}^2$, and $v_{avg} \approx \frac{v_0}{2}$. A typical 3 cm trial ($v_0 = 7\,\text{m s}^{-1}$, $h = 0.8\,\text{m}$) yielded $W_{drag} \approx 0.004\,\text{J}$. This calculated 1 % loss closely matches the observed 1 % mean loss, confirming aerodynamic drag as the primary dissipative mechanism during flight.

III. RESULTS

A. Force-displacement and work input

Table I shows the mean force at each compression, averaged across three different loadings. Force increases to a maximum of 7.1 N at 3.0 cm before declining slightly, which matches post-"pop" behavior after the spring section passes through the snap-through instability. Riemann sum integration of the mean curve gives us work values of 0.0142 J, 0.0566 J, 0.124 J and 0.155 J for four different compression levels (Table II). Mechanical work at full compression was $0.155 \pm 0.004\,\text{J}$ (Fig. 2).

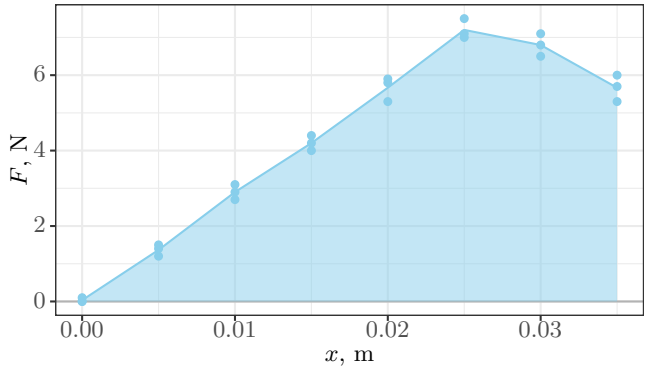

FIG. 2. Force-displacement data from Table I. The mechanical work at full compression, computed using Eq. (1) for each replicate, was 0.155 ± 0.004 J.

TABLE II. Individual trial kinematics data for launches. Values shown as mean ± sd in compact form.

x,m	v_0, m s^{-1}	h, m
0.01	1.28(2)	0.084(3)
0.02	2.66(5)	0.36(1)
0.03	3.93(8)	0.78(3)
0.04	5.00(7)	1.26(3)
0.45	5.37(9)	1.46(5)

B. Individual launch trials

Table II presents all 15 individual trials. KE and GPE are independently measured quantities.

C. Averages by compression level

Table IV summarizes the energy results by compression level. Energy loss from compression to launch (η loss) averages 46 % (Table IV). In each compression level, the three different trials are highly consistent, confirming measurement reproducibility.

A paired t-test comparing W to GPE across all 15 trials gives us $t(14) = 28.4, p < 0.0001$, confirming that the relationship between work input and launch height is statistically significant, and the null hypothesis (no relationship between work and height) is rejected.

TABLE III. Individual trial energies. Values shown as mean ± sd in compact form.

x,m	W, J	KE, J	GPE, J
0.01	0.0142	0.0047(2)	0.0047(2)
0.02	0.0566	0.0202(8)	0.0200(8)
0.03	0.124	0.044(2)	0.044(2)
0.04	0.155	0.071(2)	0.071(2)
0.45		0.082(3)	0.081(3)

TABLE IV. Mean values by compression level. Values shown as mean ± sd in compact form.

x, m	η_1	η_2	$\eta_{overall}$
0.01	0.33(1)	1.000(5)	0.33(1)
0.02	0.35(1)	0.992(1)	0.35(1)
0.03	0.36(2)	0.993(1)	0.35(1)
0.04	0.46(1)	0.9910(3)	0.46(1)
0.045		0.9920(8)	

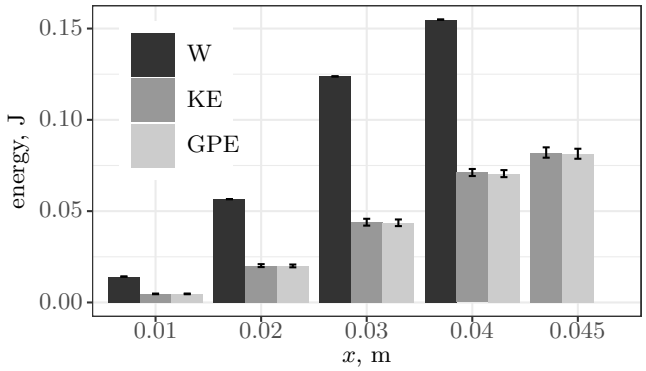

FIG. 3. Energy results by different compression levels. Data in Table III

IV. DISCUSSION

The results strongly support our hypothesis: launch height increases with work input, as do kinetic energy and maximum gravitational potential energy (Fig. 3. This confirms a robust positive correlation, not merely a trend within a single compression condition.

The mean energy efficiency $\eta = 46$ % (i.e., 54 % of compression work is lost before launch) is consistent with the literature. Gent and Cho [1] report hysteresis losses of 75 % to 88 % for rapid inversion of natural rubber shells, attributing them primarily to viscoelastic internal friction during the snap-through transition [2, 7]. Arrieta *et al.* [21]report similar values for bistable polymer shells. Our observed 54 % loss is consistent with this published range, providing quantitative support for the hysteresis mechanism. Acoustic energy loss during the snap event is estimated at less than 0.5 % of input energy and is negligible relative to hysteresis.

The secondary loss from KE to GPE averaged 1 % across all trials. Our drag estimate (Section II.E) yields a predicted loss of 1 % for mid-range trials, in good agreement with observation. This confirms that the KE-to-GPE conversion loss is physically explained by aerodynamic drag and does not represent a violation of energy conservation.

The total energy budget is therefore:

$$KE = 46\,\%W, \tag{7}$$
$$GPE = 99\,\%KE, \tag{8}$$
$$GPE = 46\,\%W. \tag{9}$$

This is fully consistent with conservation of energy when all dissipative pathways are accounted for.

Several limitations should be noted. The force-displacement curve was measured quasi-statically while the actual snap-through occurs dynamically; dynamic stiffening of rubber at high strain rates could alter the effective stored energy. Additionally, Tracker video analysis introduces pixel-level uncertainty in velocity measurement, estimated at $\pm 0.5\,\mathrm{m\,s^{-1}}$, corresponding to $\pm 1\,\%$ uncertainty in KE. Future experiments could vary what the popper dimensions are and material to explore how hysteresis fraction depends on shell thickness and elastomer composition.

V. ACKNOWLEDGEMENTS

We thank the Science & Engineering Magnet Program at Manalapan High School for support. DK authored the abstract and discussion, ML performed data analysis, and RDR prepared the methods and materials and references. The manuscript was improved with input from several anonymous peer reviewers whom we thank.

[1] A. N. Gent and I. S. Cho, Surface instabilities in compressed or bent rubber blocks, Rubber Chemistry and Technology **72**, 253 (1999).
[2] Y. Forterre, J. M. Skotheim, J. Dumais, and L. Mahadevan, How the Venus flytrap snaps, Nature **433**, 421 (2005).
[3] P. A. Tipler and G. Mosca, *Physics for Scientists and Engineers*, 5th ed. (W H Freeman and Company, New York, 2004).
[4] R. A. Pelcovits and J. Farkas, *Barron's AP Physics C Premium* (Kaplan North America, Fort Lauderdale, FL, 2024).
[5] W. Moebs, S. J. Ling, and J. Sanny, *University Physics*, Vol. 1 (OpenStax, Houston, TX, 2016).
[6] B. N. J. Persson, Rubber friction: role of the flash temperature, Journal of Physics: Condensed Matter **18**, 7789 (2006).
[7] M. Gomez, D. E. Moulton, and D. Vella, Critical slowing down in purely elastic 'snap-through' instabilities, Nature Physics **13**, 142 (2017).
[8] R. Larson and R. P. Hostetler, *Calculus*, 8th ed. (Brooks Cole, Pacific Grove, CA, 2005).
[9] D. Brown, R. Hanson, and W. Christian, Tracker video analysis and modeling tool (2025), version 6.3.3.
[10] J. Renika, E. C. Prima, and A. Amprasto, Kinematic analysis on accelerated motion using Tracker video analysis for educational purposes, Momentum Physics Education Journal **8**, 23 (2024).
[11] M. Levine, D. Khettry, K. Coulanges, and R. A. A. Dela Rosa, Acceleration is constant during free fall, Journal of Science & Engineering **2**, 41 (2026).
[12] S. Dakwale, S. Hein, R. Wallace, and S. Yellapragada, The effect of initial vertical position on velocity at which an object strikes the ground, Journal of Science & Engineering **2**, 35 (2026).
[13] I. Sharma, B. DeMairo, and A. Liddawi, Analyzing Gallileo's distance-time relationship for rolling motion on an inclined plane, Journal of Science & Engineering **2**, 38 (2026).
[14] O. Ahmadzada, J. Pawelek, M. Butch, and T. Chung, Downward acceleration is independent of mass during free fall, Journal of Science & Engineering **2**, 44 (2026).
[15] A. Hallur, J. Chan, M. Reznik, P. Zlotnikov, and J. Tiboni, Objects fall with constant acceleration regardless of mass, Journal of Science & Engineering **2**, 53 (2026).
[16] L. Brunie, J. Kadan, E. Sobel, and T. Ramesh, Testing the independence of gravitational acceleration from mass: a comparative analysis of free-falling objects near earth's surface, Journal of Science & Engineering **2**, 50 (2026).
[17] R Core Team, *R: A Language and Environment for Statistical Computing*, R Foundation for Statistical Computing, Vienna, Austria (2025).
[18] D. S. Starnes, J. Tabor, D. Yates, and D. S. Moore, *The Practice of Statistics*, 5th ed. (W. H. Freeman and Company, 2015).
[19] H. Wickham, *ggplot2: Elegant Graphics for Data Analysis* (Springer-Verlag New York, 2016).
[20] H. Wickham, R. François, L. Henry, K. Müller, and D. Vaughan, *dplyr: A Grammar of Data Manipulation* (2026), R package version 1.2.0.
[21] A. F. Arrieta, P. Hagedorn, A. Erturk, and D. J. Inman, A piezoelectric bistable plate for nonlinear broadband energy harvesting, Applied Physics Letters **97**, 104102 (2011).